Original Research Article

Applications of fractional time delayed grey model in primary energy consumption prediction

Abstract

The prediction of total energy consumption is crucial across various domains including the economy, environment, market, and geopolitics. Accurate forecasts can guide policy-making, investment decisions, and international strategies, contributing to sustainable development and energy security. Fractional models have been proven to better capture the long-term memory effects and complex dynamic characteristics of systems, with time delay playing a crucial role in capturing dynamic behaviors. Such models enhance the accuracy and reliability of predicting future trends and behaviors. For the prediction of primary energy consumption in South and Central America, the Middle East, and Africa, this study opts for the existing fractional time delayed grey model, optimizing the fractional order using the particle swarm optimization algorithm. Experimental results demonstrate that in most cases, the predictive capability of the fractional time delayed grey model surpasses that of other grey models. This indicates the effectiveness and reliability of the model in forecasting energy consumption, providing valuable references and foundations for decision-making in relevant fields.

Keywords: fractional order; time delayed; grey model; primary energy consumption

1 Introduction

The increasing global emphasis on sustainable development and environmental protection underscores the growing importance of predicting total primary energy consumption. Present-day society is confronted with multiple challenges such as climate change, energy supply security, and economic stability. Therefore, accurately understanding the trends and scale of energy consumption is crucial for formulating comprehensive energy policies. This not only helps ensure adequate and stable energy supply but also fosters the development of renewable energy, reduces reliance on fossil fuels,

lowers greenhouse gas emissions, and thus contributes to achieving global sustainable development goals.

In the field of energy consumption forecasting, the prediction time span is typically divided into three categories: long-term, medium-term, and short-term. Long-term [1, 2] forecasts usually encompass annual predictions and are utilized for formulating long-range energy policies and planning. Medium-term [3, 4, 5] forecasts include monthly and quarterly predictions, offering more flexible decision support. Short-term [6, 7, 8] forecasts, on the other hand, involve intervals such as sub-hourly, hourly, daily, and weekly, playing a crucial role in adjusting real-time energy supply and demand. Regarding the selection of prediction models, there are primarily three types: statistical (or empirical) models, machine learning models, and grey system models. Statistical models are based on linear assumptions and, although simple and user-friendly, are susceptible to overfitting or underfitting. Machine learning models can handle nonlinear time series but demand high quantities and quality of training data and require high-performance hardware. Moreover, complex parameter tuning is necessary to avoid overfitting issues. In addition to these common prediction models, there are alternative methods such as system dynamics[9, 10], Granger causality analysis[11], and hybrid forecasting systems[12]. While these methods may offer more accurate predictions in specific circumstances, they also require reliable data support. Due to limited data collection and the need to rely on recent years' data to ensure prediction reliability, researchers typically opt for small-sample prediction models (grey prediction models) when forecasting primary energy consumption.

Grey prediction theory is an effective method for modeling and forecasting in situations where data is insufficient and information is incomplete. Proposed by Professor Deng Julong [13] in 1982, it is particularly suitable for scenarios with small sample sizes, nonlinearity, and high uncertainty. The core idea of grey prediction theory is to divide known data sequences into known (white) and unknown (grey) parts, and then use the regularity of known data to predict the trend of unknown data. Grey prediction commonly employs grey differential equations or grey models to describe the development patterns of data sequences. Professor Deng Julong subsequently introduced the grey first-order (GM(1, 1)) [13] model and the grey first-order cumulative (GM(1, N)) [13] model. Many models based on Deng's ideas have since been proposed. Wang [14] combined seasonal factors with the GM(1, 1) model to develop the DSGM(1, 1) model, which was used to forecast solar energy consumption data, demonstrating its effectiveness in identifying dynamic changes caused by seasonal factors. Xia [15] improved the accumulated generating operator (AGO) to the cyclic accumulated generating operator (CAGO) to develop the SDGM model. Building upon Xia's work, Wang [16] introduced a spatial weighting matrix to create the SDGM(1, 1, m) model. As research progresses, it becomes evident that such models struggle to effectively handle nonlinear data in the real world.

Wu $et\ al.$ [17] were the first to integrate fractional orders into grey models, providing a thorough discussion on its characteristics alongside comprehensive numerical examples. These examples underscored that fractional grey models outperform traditional ones, yielding more precise forecasts for real-world scenarios. In 2019, Wu $et\ al.$ [18] introduced a groundbreaking Fractional Accumulated Nonlinear Grey Bernoulli Model (FANGBM(1, 1) model), which proved effective in addressing nonlinear sequences. Following this, Ma $et\ al.$ [19] proposed a fractional time delayed grey model (FTDGM(1, 1)), demonstrating that fractional time delay terms offer enhanced modeling flexibility and accuracy. These models exemplify the pivotal role of fractional orders and time delay terms in refining the accuracy of grey model predictions, thereby advancing the precision of grey prediction model modeling.

Fractional models have been shown to exhibit stronger adaptability when dealing with nonlinear and uncertain problems compared to traditional integer-order models. Fractional models are better equipped to capture long-term memory effects and complex dynamic characteristics of systems. Therefore, they possess greater expressive power and applicability in modeling and predicting data with nonlinear features and time delays. Additionally, time-delay terms play a crucial role in capturing the dynamic behavior of systems, enabling models to more accurately forecast future trends and behaviors. Consequently, in this study, the FTDGM(1, 1) model proposed by Ma 2 is chosen to predict the primary energy consumption in South and Central America, the Middle East, and the

Africa. The particle swarm optimization algorithm is utilized to optimize the fractional order.

The rest of this article is arranged as follows. In Section 2, the fractional order delay gray model is briefly introduced. Section 3 introduces fractional-order optimization problems and algorithms for optimizing models using particle swarm optimization algorithms. Three predictive examples are given in Section 4 and conclusions are drawn in Section 5.

2 The fractional time delayed grey model

From Ref.[19], the basic form of the fractional time delayed grey model can be expressed as

$$\frac{\mathrm{d}x^{(r)}(t)}{\mathrm{d}t} + ax^{(r)}(t) = bt^{(r)} + c, r > 0, \tag{2.1}$$

where

$$t^{(r)} = \sum_{\eta=1}^{k} \binom{k-\eta+r-1}{k-\eta} \eta. \tag{2.2}$$

Eq.(2.1) is called as the whitening equation of the model, and the discretized difference equation can be expressed as

$$x^{(r)}(k) - x^{(r)}(k-1) + az^{(r)}(k) = \frac{b}{2}\left[(k)^{(r)} + (k-1)^{(r)}\right] + c, \tag{2.3}$$

where

$$z^{(r)}(k) = \frac{1}{2}[x^{(r)}(k) + x^{(r)}(k-1)], k = 2, 3, \ldots, n \tag{2.4}$$

is the blackground value of the FTDGM(1, 1) model.

Given the fractional order r, we need to solve for the parameters a, b and c using the least squares method or the least norm method,

$$u = [a, b, c]^T = \begin{cases} (B^T B)^{-1} B^T Y, \vartheta \geq 4 \\ B^T (B^T B)^{-1} Y, \vartheta < 4 \end{cases}, \tag{2.5}$$

where

$$B = \begin{bmatrix} -z^r(2) & \frac{r+3}{2} & 1 \\ -z^r(3) & \frac{r^2+7r+10}{4} & 1 \\ \vdots & \vdots & \vdots \\ -z^r(\vartheta) & \frac{\vartheta^{(r)}+(\vartheta-1)^{(r)}}{2} & 1 \end{bmatrix}, Y = \begin{bmatrix} x^{(r)}(2) - x^{(r)}(1) \\ x^{(r)}(3) - x^{(r)}(2) \\ \vdots \\ x^{(r)}(\vartheta) - x^{(r)}(\vartheta-1) \end{bmatrix}, \tag{2.6}$$

and ϑ represents the number of modeling points.

Set initial condition $x^{(r)}(1) = x^{(0)}(1)$, and then combine the constant variation method and the trapezoid formula, the discrete response function of the solution can be written as

$$\hat{x}^{(r)}(k) = x^{(0)}(1)e^{-a(k-1)} + \sum_{\tau=2}^{k} \left\{ e^{-a(k-\tau+\frac{1}{2})} \frac{1}{2} [f(\tau) + f(\tau-1)] \right\}, k = 2, \ldots, n, \tag{2.7}$$

where $f(\tau) = b\tau^{(r)} + c$.

Therefore, the restored values $\hat{x}^{(0)}$ can be easily obtained as

$$\hat{x}^{(0)}(k) = \sum_{\eta=1}^{k} \binom{k-\eta-r-1}{k-\eta} \hat{x}^{(r)}(\eta). \tag{2.8}$$

3 Optimization of fractional order by the Particle Swarm Optimization

The previous section introduced the FTDGM(1, 1) model. Since the fractional order r directly influences the accuracy and predictive capability of the model, it plays a crucial role in both model establishment and solution. Therefore, this section focuses on addressing the nonlinear constrained optimization problem aimed at optimizing the fractional order r.

3.1 Establishing an optimization problem to optimize the fractional order

In the quest for the optimal fractional order r, the primary objective is to minimize the fractional time delayed grey model's error. The choice of error evaluation criteria significantly impacts the performance of optimization algorithms and the overall quality of the model. For the fractional time delayed grey model (FTDGM(1, 1)), commonly used error evaluation methods include Mean Squared Error (MSE), Root Mean Squared Error (RMSE), Mean Absolute Error (MAE), and Mean Absolute Percentage Error (MAPE), among others. Given MAPE's interpretability and its resilience to outliers, this study selects it as the primary evaluation criterion. MAPE, utilized during both fitting and prediction phases, is expressed by the following formulas to comprehensively assess the model's fitting and predictive performance. The adoption of MAPE not only offers a clear metric for model accuracy but also provides a reliable foundation for further analysis to optimize model parameters and enhance predictive outcomes.

$$MAPE_{fit} = \frac{1}{\vartheta}\sum_{k=1}^{\vartheta}\left|\frac{\hat{x}^{(0)}(k)-x^{(0)}(k)}{x^{(0)}(k)}\right| \times 100\%, \tag{3.1}$$

$$MAPE_{pred} = \frac{1}{n-\vartheta}\sum_{k=1}^{n-\vartheta}\left|\frac{\hat{x}^{(0)}(k)-x^{(0)}(k)}{x^{(0)}(k)}\right| \times 100\%, \tag{3.2}$$

where, ϑ represents the number of modeling points, and n represents the total number of data points.

$$\min J(r) = \frac{1}{\vartheta}\sum_{k=1}^{\vartheta}\left|\frac{\hat{x}^{(0)}(k)-x^{(0)}(k)}{x^{(0)}(k)}\right| \times 100\%$$

$$\text{s.t.}\begin{cases} (a,b,c)^T = (B^TB)^{-1}B^TY, & \vartheta \geq 4 \\ (a,b,c)^T = B^T(B^TB)^{-1}Y, & \vartheta < 4 \\ B = \begin{bmatrix} -z^r(2) & \frac{r+3}{2} & 1 \\ -z^r(3) & \frac{r^2+7r+10}{4} & 1 \\ \vdots & \vdots & \vdots \\ -z^r(\vartheta) & \frac{\vartheta^{(r)}+(\vartheta-1)^{(r)}}{2} & 1 \end{bmatrix} \\ Y = \left[x^{(r)}(2)-x^{(r)}(1), x^{(r)}(3)-x^{(r)}(2), \ldots, x^{(r)}(\vartheta)-x^{(r)}(\vartheta-1)\right]^T \\ z^{(r)}(k) = \frac{1}{2}[x^{(r)}(k)+x^{(r)}(k-1)], \quad k=2,\ldots,n \\ \hat{x}^{(r)}(k) = x^{(0)}(1)e^{-a(k-1)} + \sum_{\tau=2}^{k}\left\{e^{-a(k-\tau+\frac{1}{2})}\frac{1}{2}\left[f(\tau)+f(\tau-1)\right]\right\} \\ f(\tau) = b\tau^{(r)}+c \\ \hat{x}^{(0)}(k) = \sum_{\eta=1}^{k} C_{k-\eta-r-1}^{k-\eta}\hat{x}^{(0)}(\eta), \quad k=2,\ldots,n \end{cases}, \tag{3.3}$$

The objective of this study is to iteratively adjust the fractional order r within a specified range to minimize the discrepancy between model predictions and actual observations. The optimization

problem outlined above is evidently a complex nonlinear optimization problem characterized by multiple nonlinear constraints, owing to the complexity of the underlying system dynamics. To address this challenge, advanced optimization techniques are employed in this study, utilizing the particle swarm optimization algorithm (PSO) to handle the nonlinear constraints effectively.

3.2 The Particle Swarm Optimization

The Particle Swarm Optimization (PSO) is an optimization algorithm based on swarm intelligence, inspired by the collective behavior of organisms such as bird flocks or fish schools. The algorithm was initially proposed by Kennedy and Eberhart in 1995, based on the simulation of foraging behavior in bird flocks.

The core idea of the PSO is to simulate the cooperation and competition among individuals within a bird flock, continuously updating the positions and velocities of particles to search for the optimal solution to a problem. In PSO, each candidate solution is represented as a particle, which moves in the solution space and adjusts its movement based on its individual experience and the collective experience of the group. The movement of particles is governed by two important information update rules. Firstly, the Personal Best (Local Optimum), where each particle remembers the best position it has encountered during its search process. Secondly, the Global Best (Global Optimum), which represents the position of the best solution among all particles. The key aspect of the PSO algorithm lies in how to update the velocities and positions of particles. One common updating method is based on the following formula,

$$\begin{cases} v_i^{t+1} = w \cdot v_i^t + c_1 \cdot rand_1 \cdot (pbest_i - x_i^t) + c_2 \cdot rand_2 \cdot (gbest - x_i^t) \\ x_i^{t+1} = x_i^t + v_i^{t+1} \end{cases}, \tag{3.4}$$

where v_i^t is the velocity of particle i at time t, x_i^t is the position of particle i at time t, $pbest_i$ is the personal best position of particle i, $gbest$ is the global best position of the entire group, w is the inertia weight, c_1 and c_2 are acceleration factors, and $rand_1$ and $rand_2$ are random numbers between 0 and 1. By continuously updating the velocities and positions of particles, the PSO algorithm is able to effectively search and converge to the optimal solution in the solution space. This algorithm is characterized by its simplicity, ease of implementation, and efficiency, hence it has been widely applied in various optimization problems.

3.3 Computational details

Appropriate parameter configuration is crucial for accurately fitting empirical data. The constrained optimization problem 3.3 is evidently a complex nonlinear problem, with the explicit formulation of its constraints posing a challenge. Therefore, ths study choose to validate the constraints in the particle swarm optimization algorithm, as detailed in 1. The implementation of 1 is based on Python source code using the pyswarm library, which can be accessed at https://github.com/tisimst/pyswarm.

Algorithm 1: The algorithm for solving the optimization problem

input : The initial sequence $x^{(0)} = \left(x^{(0)}(1), x^{(0)}(2), \ldots, x^{(0)}(n)\right)$
output: The fractional oreder (r^*)

Set max iteration = 100
Initialize $(\text{MAPE}_{fit})_{\min} = \inf$, the best agent of r
for r in agent, len = max iteration **do**
    Construst B and Y by the Eq.(2.6)
    Compute a, b, c by the Eq.(2.5)
    for $k = 1$ to n, step = 1 **do**
        Compute $\hat{x}^{(r)}(k)$ by the Eq.(2.7)
        Compute $\hat{x}^{(0)}(k)$ by the Eq.(2.8)
    end
    Compute MAPE_{fit} using the objective function in Eq.(3.1)
    if $\text{MAPE}_{fit} < (\text{MAPE}_{fit})_{\min}$ **then**
        $(\text{MAPE}_{fit})_{\min} \leftarrow \text{MAPE}_{fit}$
        $r^* \leftarrow r$
    end
end

4 Applications in forecasting primary energy consumption

4.1 Preparation

Accurately predicting primary energy consumption is crucial for South and Central America, the Middle East, and the Africa. Primary energy plays a vital role in the economies, industries, and daily lives of these regions. In South and Central America, as well as in the Middle East and Africa, primary energy consumption is closely tied to industrialization, urbanization, and transportation. Accurate forecasts of energy consumption trends can assist governments and businesses in planning energy supply and transitions, thereby promoting sustainable development and environmental protection. The Middle East, being a significant global energy exporter, relies heavily on primary energy sources such as oil and natural gas, which serve as the backbone of the region's economy. Accurately predicting the consumption trends of these energy sources is crucial for maintaining energy stability and fostering economic development. In Africa, primary energy consumption is closely linked to issues of energy scarcity and poverty. Accurately forecasting primary energy consumption trends can help address energy security issues, stimulate economic development, and improve people's quality of life. Therefore, accurate predictions of primary energy consumption in South and Central America, the Middle East, and Africa are essential for energy security, economic development, and sustainable growth in these regions.

For this research, raw data has been sourced from the Energy Institute (EI) Statistical Review of World Energy, accessible at https://www.energyinst.org/statistical-review (accessed on 28 March 2024). Data on annual primary energy consumption in South and Central America, the Middle East, and the Africa were collected, covering the period from 2000 to 2022. Data from 2000 to 2015 were designated as the sample set for constructing the grey model. Meanwhile, data from 2016 to 2022 were used to test the out-of-sample performance of the model, effectively verifying the model's generalization ability. This approach allows for a more comprehensive evaluation of the model's predictive performance regarding future trends.

Table 1. Model performance metrics.

Metrics	Abbreviation	Formula
Average Relative Error	ARE	$\frac{1}{n}\sum_{k=1}^{n}\left\lvert\frac{x^{(0)}(k)-\hat{x}^{(0)}(k)}{x(k)}\right\rvert$
Mean Absolute Error	MAE	$\frac{1}{n}\sum_{k=1}^{n}\left\lvert x^{(0)}(k)-\hat{x}^{(0)}(k)\right\rvert$
Mean Absolute Percentage Error	MAPE	$\frac{1}{n}\sum_{k=1}^{n}\left\lvert\frac{x^{(0)}(k)-\hat{x}^{(0)}(k)}{x(k)}\right\rvert\times 100\%$
Mean Percentage Error	MPE	$\frac{1}{n}\sum_{k=1}^{n}\frac{x^{(0)}(k)-\hat{x}^{(0)}(k)}{x(k)}\times 100\%$
Mean Arctangent Absolute Percentage Error	MAAPE	$\frac{1}{n}\sum_{k=1}^{n}\arctan\left(\left\lvert\frac{x^{(0)}(k)-\hat{x}^{(0)}(k)}{x(k)}\right\rvert\right)$
Mean Square Error	MSE	$\frac{1}{n}\sum_{k=1}^{n}\left(x^{(0)}(k)-\hat{x}^{(0)}(k)\right)^2$
Root Mean Square Error	RMSE	$\sqrt{\frac{1}{n}\sum_{k=1}^{n}\left(x^{(0)}(k)-\hat{x}^{(0)}(k)\right)^2}$
Root Mean Square Percentage Error	RMSPE	$\sqrt{\frac{1}{n}\sum_{k=1}^{n}\left\lvert\frac{x^{(0)}(k)-\hat{x}^{(0)}(k)}{x(k)}\right\rvert^2}$
Symmetric Mean Absolute Percentage Error	SMAPE	$\frac{1}{n}\sum_{k=1}^{n}\left\lvert\frac{x^{(0)}(k)-\hat{x}^{(0)}(k)}{0.5x^{(0)}(k)+0.5\hat{x}^{(0)}(k)}\right\rvert\times 100\%$
Theil U Statistic 1	U1	$\frac{\sqrt{\frac{1}{n}\sum_{k=1}^{n}\left(x^{(0)}(k)-\hat{x}^{(0)}(k)\right)^2}}{\sqrt{\frac{1}{n}\sum_{k=1}^{n}\left(x^{(0)}(k)\right)^2}+\sqrt{\frac{1}{n}\sum_{k=1}^{n}\left(\hat{x}^{(0)}(k)\right)^2}}$
Theil U Statistic 2	U2	$\frac{\sqrt{\frac{1}{n}\sum_{k=1}^{n}\left(x^{(0)}(k)-\hat{x}^{(0)}(k)\right)^2}}{\sqrt{\frac{1}{n}\sum_{k=1}^{n}\left(x^{(0)}(k)\right)^2}}$
Average Error	AE	$\frac{1}{n}\sum_{k=1}^{n}\left(x^{(0)}(k)-\hat{x}^{(0)}(k)\right)$
Percent Bias	Pidas	$\frac{\sum_{k=1}^{n}\left(x^{(0)}(k)-\hat{x}^{(0)}(k)\right)}{\sum_{k=1}^{n}\hat{x}^{(0)}(k)}$

To assess the effectiveness of the fractional time delayed grey model (FTDGM(1, 1)), comprehensive comparisons of model performance were conducted against eight established benchmark grey system models. Additionally, thirteen evaluation metrics were applied to provide a thorough assessment, as shown in Table 1, offering quantitative measurements and analysis of various aspects of model performance. The benchmark grey system models involved the classical grey model (GM(1, 1)) [13], the discrete grey model (DGM(1, 1)) [20], the nonlinear grey Bernoulli model (NGBM(1, 1)) [21], the fractional-order grey model (FGM(1, 1)) [17], the fractional nonlinear grey Bernoulli model (FANGBM(1, 1)) [18], the fractional order discrete grey model (FDGM(1, 1)) [22], the fractional grey model (FAGM$(1, 1, t^{\alpha})$) [23], and the Simpson fractional grey model (SFAGM(1, 1))[24]. Furthermore, models incorporating external input parameters underwent parameter optimization using the Particle Swarm Optimization algorithm (PSO).

4.2 Forecasting results and analysis

4.2.1 Case I: Forecasting primary energy consumption in the South and Central America.

Using the primary energy consumption data from 2000 to 2022 in South and Central America, the grey model was built using data from 2000 to 2015, while data from 2016 to 2022 were utilized to test its out-of-sample performance. Figure 2 displays all predicted values of total primary energy consumption in the region. Table 2 provides the evaluation metrics of the sample population, and Table 3 lists detailed results of the model predictions. In this process, the particle swarm optimization algorithm was employed to optimize the parameters of the eight models, with the optimization results

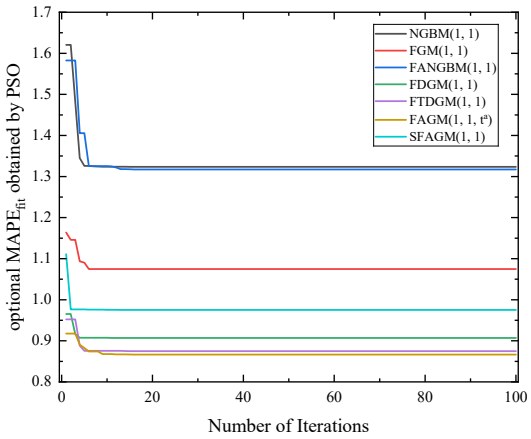

Figure 1. Optimal MAPE$_{fit}$ of model in Case I under PSO algorithm.

shown in Figure 1.

From Figure 1, it can be observed that after using the particle swarm optimization algorithm to establish the models, the MAPE$_{fit}$ of all parameter-containing grey models reached optimal values, with the FAGM(1, 1, t^{α}) model exhibiting a smaller MAPE$_{fit}$. As depicted in Figure 2, the FTDGM(1, 1) model demonstrated excellent performance in out-of-sample predictions. It can be seen that other competing models deviated significantly from the actual data, whereas only the FTDGM(1, 1) model accurately captured subtle data changes, resulting in a prediction trend that closely matched the original data. Special points observed in Figure 2 reveal that starting from 2016, particularly in 2020, the FTDGM(1, 1) model accurately captured subtle data changes, making the prediction trend even closer to the original data, while other models exhibited larger errors.

Table 2 illustrates that the evaluation metrics of the FTDGM(1, 1) model are significantly smaller than those of other models. Particularly, FTDGM(1, 1)'s MSE is the only one among all models that is less than 1. When out-of-sample MAPE$_{pre}$ was used as an evaluation metric, the FTDGM(1, 1) model performed the best in the prediction phase, with its MAPE$_{pre}$ significantly smaller than those of other competing models. The out-of-sample MAPE$_{pre}$ of the FTDGM(1, 1) model is 4.496%, the only model with an MAPE less than 5%. Table 3 clearly shows that the in-sample MAPE$_{fit}$ of the FAGM(1, 1) model is smaller than that of the FTDGM(1, 1), indicating better in-sample predictive performance, but its performance in out-of-sample prediction is poor, indicating overfitting. Therefore, in this case, the prediction results of the FTDGM(1, 1) model are closer to the original data curve, demonstrating better predictive performance.

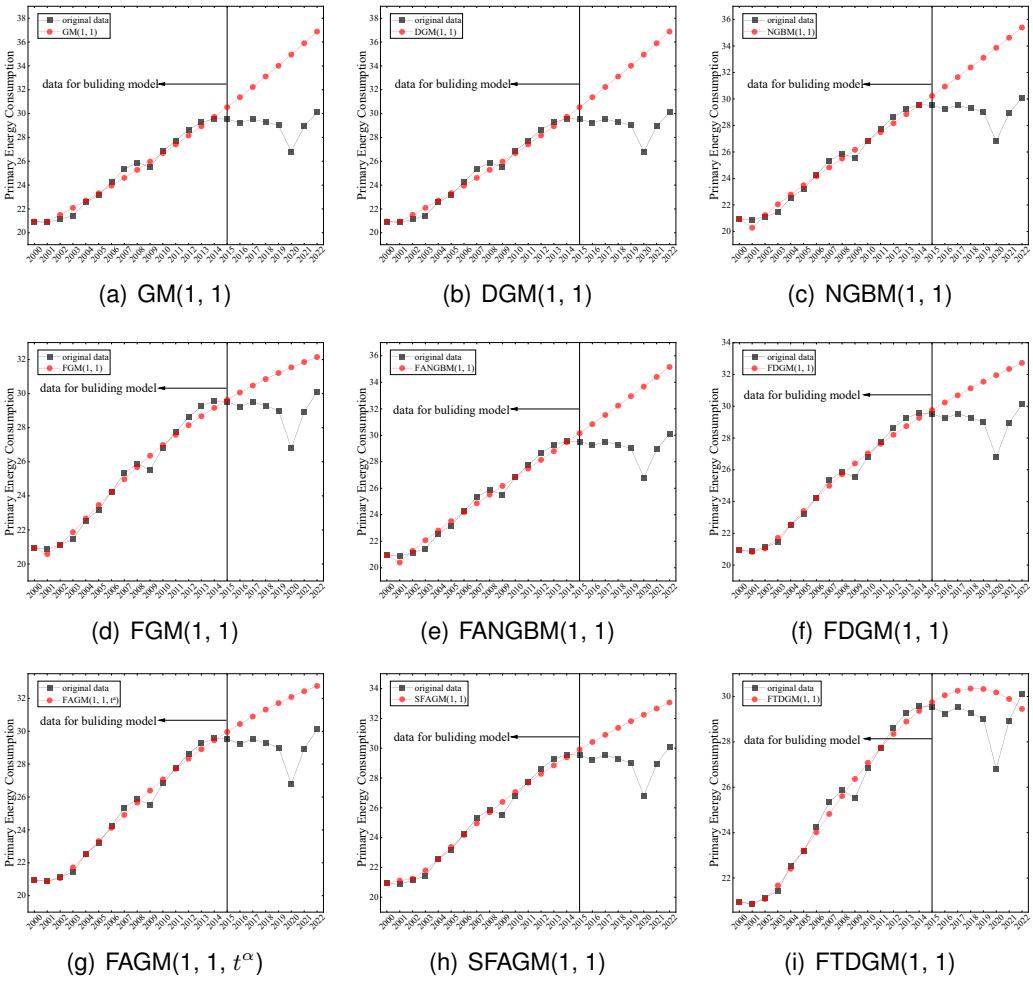

(a) GM(1, 1) (b) DGM(1, 1) (c) NGBM(1, 1)

(d) FGM(1, 1) (e) FANGBM(1, 1) (f) FDGM(1, 1)

(g) FAGM(1, 1, t^{α}) (h) SFAGM(1, 1) (i) FTDGM(1, 1)

Figure 2. Predicted values of all models in Case I.

Table 2. Overall-sample forecasting metrics for all models in Case I.

	ARE	MAE	MAPE	MPE	MAAPE	MSE	RMSE	RMSPE	SMAPE	U1	U2	AE	Pibas
GM(1, 1)	0.06371	1.799968	6.371049	-5.41735	0.062847	9.364971	3.060224	0.107555	5.861564	0.055813	0.115388	-1.54664	-0.05548
DGM(1, 1)	0.063722	1.800156	6.372203	-5.42278	0.062859	9.364384	3.060128	0.107553	5.862666	0.05581	0.115385	-1.54796	-0.05553
NGBM(1, 1)	0.053256	1.493998	5.325643	-4.40444	0.05275	6.378239	2.525518	0.089183	4.971726	0.046353	0.095227	-1.25958	-0.04565
FGM(1, 1)	0.03078	0.85553	3.077973	-2.26995	0.030671	2.005255	1.41607	0.050904	2.961998	0.026346	0.053394	-0.63828	-0.02367
FANGBM(1, 1)	0.051435	1.442209	5.14347	-4.2542	0.050978	5.909647	2.430977	0.085907	4.813632	0.044667	0.091662	-1.212	-0.04401
FDGM(1, 1)	0.03331	0.93598	3.331018	-2.69505	0.033161	2.561162	1.600363	0.057161	3.182015	0.029696	0.060343	-0.76226	-0.02814
FAGM(1, 1, t^{α})	0.034555	0.971874	3.455523	-2.91333	0.034392	2.759566	1.661194	0.059273	3.294236	0.030782	0.062637	-0.82747	-0.03047
SFAGM(1, 1)	0.03655	1.024424	3.655033	-3.14589	0.036366	3.018208	1.737299	0.061922	3.479137	0.032158	0.065506	-0.88461	-0.03251
FTDGM(1, 1)	**0.019769**	**0.545107**	**1.976882**	**-1.10286**	**0.019736**	**0.795232**	**0.891758**	**0.032585**	**1.932415**	**0.016706**	**0.033624**	**-0.30768**	**-0.01155**

Table 3. Detailed results of sample predictions for all models in Case I.

	original data	GM(1, 1)		DGM(1, 1)		NGBM(1, 1)		FGM(1, 1)		FANGBM(1, 1)		FDGM(1, 1)		FAGM(1, 1, t^{α})		SFAGM(1, 1)		FTDGM(1, 1)	
		value	error(%)	value	error(%)	value	error(%)	value	error(%)	value	error(%)	value	error(%)	value	error(%)	value	error(%)	value	error(%)
2000	20.94000	20.94000	0.00000	20.94000	0.00000	20.94000	0.00000	20.94000	0.00000	20.94000	0.00000	20.94000	0.00000	20.94000	0.00000	20.94000	0.00000	20.94000	0.00000
2001	20.87000	20.92804	0.27811	20.93088	0.29169	20.27872	2.83316	20.57534	1.41188	20.39803	2.26146	20.82511	0.21510	20.87000	0.00000	21.11739	1.18540	20.87000	0.00000
2002	21.13000	21.50043	1.75309	21.50318	1.76611	21.23822	0.51215	21.12358	0.03036	21.27015	0.66326	21.04416	0.40623	21.06929	0.28733	21.24272	0.53347	21.07863	0.24310
2003	21.44000	22.08847	3.02458	22.09113	3.03699	22.04690	2.83071	21.86987	2.00501	22.07000	2.93846	21.71577	1.28626	21.72130	1.31205	21.79248	1.64401	21.67272	1.08546
2004	22.55000	22.69259	0.63235	22.69516	0.64372	22.78627	1.04775	22.66597	0.51428	22.81140	1.15918	22.55000	0.00000	22.50234	0.21137	22.55000	0.00000	22.40898	0.62538
2005	23.19000	23.31324	0.53144	23.31570	0.54206	23.48850	1.28718	23.46135	1.17011	23.51566	1.40431	23.40375	0.92173	23.31654	0.54566	23.36856	0.76999	23.20335	0.05758
2006	24.25000	23.95086	1.23355	23.95321	1.22386	24.16979	0.33077	24.23499	0.06190	24.19667	0.21990	24.22416	0.10655	24.12553	0.51329	24.18062	0.28610	24.01580	0.96577
2007	25.34000	24.60593	2.89690	24.60815	2.88810	24.83951	1.97510	24.97744	1.43079	24.86340	1.88082	24.99643	1.35584	24.91184	1.68968	24.96015	1.49903	24.82321	2.03941
2008	25.88000	25.27890	2.32263	25.28100	2.31451	25.50361	1.45437	25.68452	0.75532	25.52188	1.38377	25.71979	0.61905	25.66716	0.82239	25.69956	0.69723	25.61024	1.04237
2009	25.52000	25.97029	1.76445	25.97225	1.77215	26.16614	2.53188	26.35473	3.27087	26.17637	2.57199	26.39799	3.44042	26.38769	3.40005	26.39876	3.44340	26.36540	3.31270
2010	26.83000	26.68058	0.55691	26.68240	0.55013	26.83000	0.00000	26.98794	0.58867	26.83000	0.00001	27.03581	0.76708	27.07196	0.90182	27.06037	0.85863	27.07931	0.92920
2011	27.74000	27.41030	1.18853	27.41196	1.18254	27.49738	0.87462	27.58485	0.55931	27.48515	0.91870	27.63781	0.36840	27.71981	0.07280	27.68777	0.18828	27.74364	0.01311
2012	28.63000	28.15998	1.64171	28.16148	1.63648	28.16997	1.60680	28.14656	1.68858	28.14369	1.69861	28.20805	1.47382	28.33181	1.04152	28.28430	1.20747	28.35060	0.97590
2013	29.26000	28.93016	1.12727	28.93148	1.12275	28.84915	1.40414	28.67443	2.00125	28.80712	1.54779	28.75001	1.74295	28.90898	1.19964	28.85303	1.39087	28.89258	1.25572
2014	29.57000	29.72141	0.51203	29.72254	0.51587	29.53603	0.11488	29.16994	1.35291	29.47669	0.31556	29.26669	1.02573	29.45256	0.39717	29.39667	0.58616	29.36188	0.70382
2015	29.53000	30.53430	3.40093	30.53523	3.40411	30.23158	2.37582	29.63461	0.35426	30.15346	2.11126	29.76062	0.78098	29.96389	1.46931	29.91759	1.31254	29.75059	0.74702
MAPE$_{fit}$			1.42903		1.43069		1.32371		1.07472		1.31719		0.90688		**0.86651**		0.97516		0.87478
2016	29.24000	31.36942	7.28254	31.37014	7.28503	30.93662	5.80241	30.06997	2.83846	30.83833	5.46625	30.23399	3.39942	30.44439	4.11898	30.41787	4.02827	30.05043	2.77166
2017	29.52000	32.22738	9.17133	32.22788	9.17305	31.65190	7.22187	30.47751	3.24360	31.53211	6.81610	30.68868	3.95894	30.89549	4.65952	30.89929	4.67241	30.25264	2.48185
2018	29.29000	33.10880	13.03791	33.10908	13.03884	32.37806	10.54305	30.85871	5.35579	32.23552	10.05640	31.12631	6.26942	31.31859	6.92588	31.36345	7.07905	30.34789	3.61177
2019	29.01000	34.01434	17.25038	34.01436	17.25047	33.11572	14.15276	31.21498	7.60075	32.94921	13.57878	31.54832	8.74979	31.71507	9.32461	31.81173	9.65782	30.32618	4.53698
2020	26.81000	34.94464	30.34180	34.94440	30.34092	33.86542	26.31639	31.54767	17.67128	33.67377	25.60151	31.95594	19.19409	32.08525	19.68016	32.24536	20.27362	30.17678	12.55791
2021	28.93000	35.90038	24.09395	35.89987	24.09219	34.82771	19.69483	31.85808	10.12127	34.40976	18.94145	32.35027	11.82257	32.43342	12.11000	32.66541	12.91189	29.88810	3.31178
2022		36.88226	22.49174	36.88146	22.48909	35.40308	17.57914	32.14746	6.76672	35.15772	16.76425	32.73229	8.70905	32.75781	8.79378	33.07286	9.84011	29.44765	2.19978
MAPE$_{pre}$			17.66709		17.66708		14.47292		7.65684		13.88925		8.87190		9.37327		9.78045		**4.49596**

4.2.2 Case II: Forecasting primary energy consumption in the Middle East.

The primary energy consumption data from 2000 to 2022 in Africa were utilized. The first 16 data points were used for constructing the grey model, while the remaining data were employed to test its out-of-sample performance. All predicted values of the primary energy consumption in Africa are illustrated in Figure 4. Table 4 provides the evaluation metrics of the sample population. Table 5 presents detailed results of the model predictions. The results of optimizing model parameters using the particle swarm optimization algorithm are shown in Figure 3.

From Figure 3, it can be observed that the MAPE$_{fit}$ of the grey model optimized using the particle swarm optimization algorithm reached the optimal values. Similarly, the FAGM(1, 1, t^{α}) model exhibited a smaller MAPE$_{fit}$, while the FDGM(1, 1) model's MAPE$_{fit}$ was close to that of the FTDGM(1, 1) model. According to Figure 4, the predictive performance of the nine models was similar in-sample, but in out-of-sample predictions, the FTDGM(1, 1) model clearly demonstrated better trends, closely resembling the original data.

Table 4 shows that the evaluation metrics of the FTDGM(1, 1) model are significantly lower than those of other models. Interestingly, the FTDGM(1, 1) model's metrics are almost over five times smaller than the maximum metric value among other models. When out-of-sample MAPE$_{pre}$ is used as an evaluation metric, the FTDGM(1, 1) model has the smallest MAPE$_{pre}$ value, at 3.179%. From Table 5, it can be seen that the out-of-sample MAPE$_{pre}$ of GM(1, 1) and DGM(1, 1) are 17.11% and 17.14%, respectively, which are much larger than that of the FTDGM(1, 1) model, indicating that linear models do not accurately capture the turning points in the data. Although the FAGM(1, 1, t^{α}) model has a smaller in-sample MAPE than the FTDGM model, its out-of-sample MAPE$_{pre}$ is greater than that of the FTDGM(1, 1) model, indicating overfitting. Therefore, in this case, the FTDGM(1, 1) model performs better.

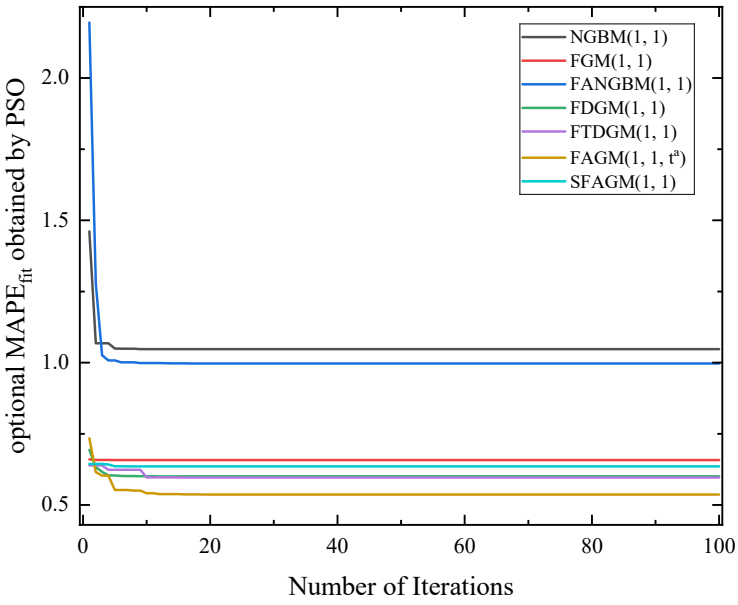

Figure 3. Optimal MAPE$_{fit}$ of model in Case II under PSO algorithm.

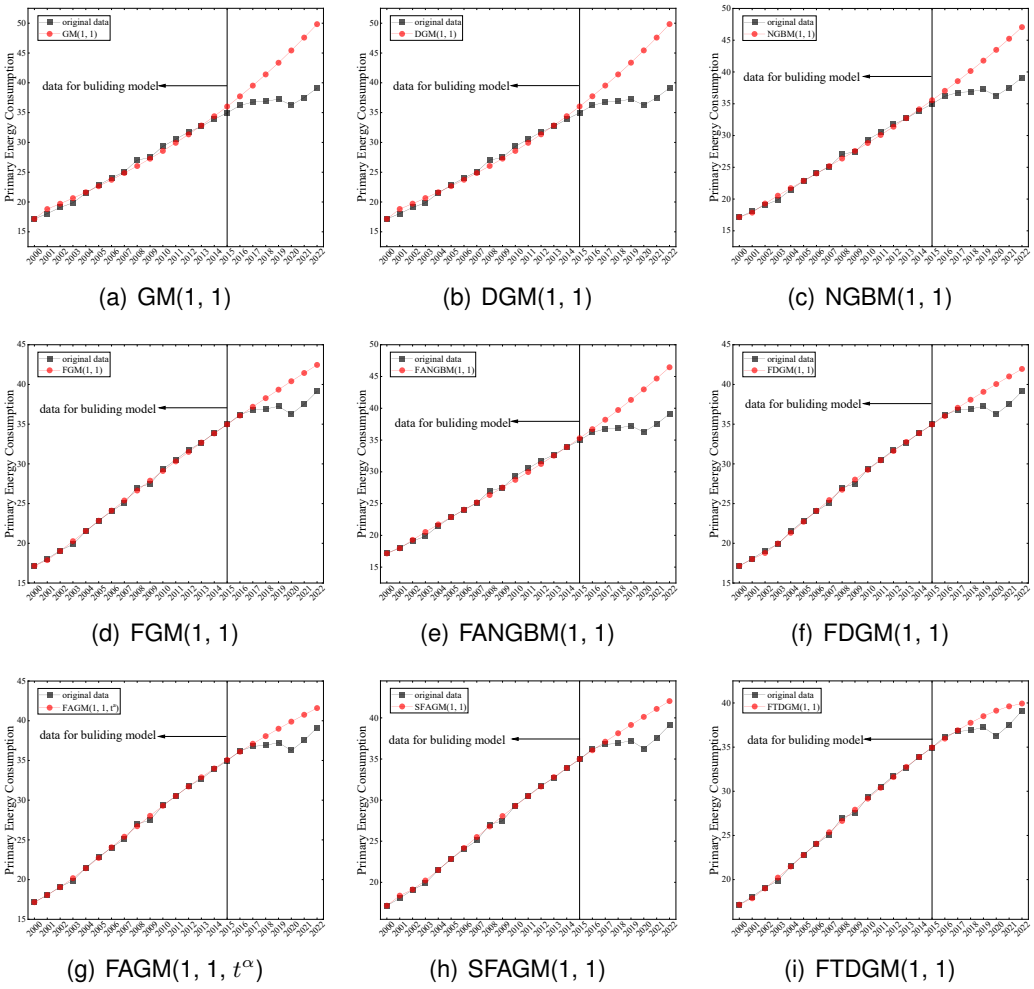

(a) GM(1, 1) (b) DGM(1, 1) (c) NGBM(1, 1)

(d) FGM(1, 1) (e) FANGBM(1, 1) (f) FDGM(1, 1)

(g) FAGM(1, 1, t^{α}) (h) SFAGM(1, 1) (i) FTDGM(1, 1)

Figure 4. Predicted values of all models in Case II.

Table 4. Overall-sample forecasting metrics for all models in Case II.

	ARE	MAE	MAPE	MPE	MAAPE	MSE	RMSE	RMSPE	SMAPE	U1	U2	AE	Pibas
GM(1, 1)	0.065247	2.284591	6.524715	-5.37058	0.064369	16.21278	4.02651	0.108046	6.014672	0.063958	0.133375	-1.96353	-0.06268
DGM(1, 1)	0.065315	2.286991	6.531529	-5.39568	0.064434	16.24908	4.031015	0.108171	6.020016	0.064022	0.133524	-1.97089	-0.0629
NGBM(1, 1)	0.045935	1.637137	4.593466	-3.91014	0.045543	9.20039	3.033214	0.081174	4.297273	0.048716	0.100473	-1.44814	-0.047
FGM(1, 1)	0.022487	0.78411	2.248686	-1.77504	0.022436	2.213049	1.487632	0.040222	2.173547	0.024303	0.049277	-0.65577	-0.02185
FANGBM(1, 1)	0.041798	1.486509	4.179794	-3.4045	0.041489	7.776134	2.788572	0.074696	3.929889	0.044956	0.092369	-1.26224	-0.04122
FDGM(1, 1)	0.019966	0.692741	1.996601	-1.49923	0.01993	1.740282	1.319197	0.035749	1.93753	0.021587	0.043697	-0.57006	-0.01904
FAGM(1, 1, t^{α})	0.018479	0.646758	1.847864	-1.61898	0.018449	1.516952	1.231646	0.03344	1.794831	0.020155	0.040797	-0.58704	-0.0196
SFAGM(1, 1)	0.020642	0.712899	2.064175	-1.90946	0.020603	1.836923	1.355331	0.036863	1.999436	0.022149	0.044894	-0.66625	-0.02219
FTDGM(1, 1)	**0.013824**	**0.461265**	**1.382396**	**-0.91617**	**0.013813**	**0.710082**	**0.842664**	**0.023439**	**1.357643**	**0.013859**	**0.027913**	**-0.3381**	**-0.01138**

Table 5. Detailed results of sample predictions for all models in Case II.

	original data	GM(1, 1)		DGM(1, 1)		NGBM(1, 1)		FGM(1, 1)		FANGBM(1, 1)		FDGM(1, 1)		FAGM(1, 1, t^{α})		SFAGM(1, 1)		FTDGM(1, 1)	
		value	error(%)	value	error(%)	value	error(%)	value	error(%)	value	error(%)	value	error(%)	value	error(%)	value	error(%)	value	error(%)
2000	17.16000	17.16000	0.00000	17.16000	0.00000	17.16000	0.00000	17.16000	0.00000	17.16000	0.00000	17.16000	0.00000	17.16000	0.00000	17.16000	0.00000	17.16000	0.00000
2001	18.06000	18.82005	4.20845	18.82585	4.24060	17.86657	1.07106	17.88208	0.98514	17.97555	0.46760	18.01160	0.26797	18.05600	0.02217	18.38095	1.77714	17.88691	0.95841
2002	19.09000	19.71342	3.26571	19.71940	3.29701	19.28682	1.03103	19.02757	0.32701	19.28981	1.04670	18.79021	1.57038	19.04868	0.21642	19.13100	0.21476	18.99752	0.48446
2003	19.87000	20.64921	3.92154	20.65535	3.95247	20.53576	3.35058	20.27518	2.03915	20.53240	3.33365	19.97212	0.51393	20.18861	1.60347	20.22175	1.77027	20.21783	1.75051
2004	21.50000	21.62942	0.60195	21.63574	0.63133	21.71814	1.01459	21.55442	0.25312	21.72064	1.02622	21.32322	0.82222	21.43146	0.31877	21.50000	0.00000	21.48390	0.07487
2005	22.84000	22.65616	0.80492	22.66265	0.77650	22.87573	0.15642	22.84000	0.00000	22.88042	0.17697	22.71382	0.55246	22.73486	0.46032	22.84088	0.00384	22.77050	0.30429
2006	24.03000	23.73163	1.24164	23.73830	1.21389	24.03000	0.00000	24.12059	0.37698	24.03000	0.00000	24.09185	0.25740	24.06636	0.15133	24.18552	0.64720	24.06443	0.14329
2007	25.09000	24.85816	0.92402	24.86501	0.89673	25.19380	0.41373	25.39045	1.19750	25.18206	0.36692	25.43852	1.38907	25.40245	1.24531	25.50950	1.67198	25.35728	1.06529
2008	27.03000	26.03817	3.66938	26.04520	3.64337	26.37572	2.42059	26.64648	1.41887	26.34580	2.53127	26.74806	1.04305	26.72650	1.12284	26.80358	0.83768	26.64270	1.43284
2009	27.48000	27.27419	0.74896	27.28140	0.72271	27.58195	0.37101	27.88692	1.48079	27.52822	0.17548	28.01985	1.96452	28.02706	1.99075	28.06501	2.12886	27.91522	1.58376
2010	29.34000	28.56888	2.62822	28.57628	2.60301	28.81736	1.78133	29.11078	0.78124	28.73494	2.06224	29.25521	0.28899	29.29650	0.14825	29.29383	0.15735	29.16958	0.58083
2011	30.53000	29.92503	1.98156	29.93261	1.95672	30.08590	1.45463	30.31753	0.69593	29.97062	1.83223	30.45619	0.24175	30.53000	0.00000	30.49123	0.12698	30.40042	0.42444
2012	31.75000	31.34556	1.27384	31.35333	1.24936	31.39101	1.13069	31.50691	0.76564	31.23932	1.60844	31.62504	0.39359	31.72476	0.07949	31.65885	0.28710	31.60190	0.46645
2013	32.68000	32.83351	0.46975	32.84148	0.49411	32.73574	0.17056	32.67883	0.00358	32.54467	0.41411	32.76393	0.25684	32.87948	0.61041	32.79844	0.36241	32.76755	0.26790
2014	33.89000	34.39211	1.48157	34.40025	1.50562	34.12292	0.68729	33.83333	0.16721	33.89000	0.00000	33.87495	0.04440	33.99392	0.30664	33.91174	0.06416	33.89000	0.00000
2015	34.96000	36.02468	3.04543	36.03302	3.06928	35.55523	1.70261	34.97052	0.03009	35.27845	0.91091	34.96000	0.00000	35.06858	0.31058	35.00042	0.11563	34.96079	0.00226
MAPE$_{fit}$			1.89168		1.89079		1.04726		0.65764		0.99705		0.60041		**0.53667**		0.63533		0.59622
2016	36.20000	37.73476	4.23966	37.74328	4.26321	37.03524	2.30729	36.09056	0.30232	36.71305	1.41726	36.02081	0.49500	36.10448	0.26388	36.06601	0.37013	35.97011	0.63505
2017	36.77000	39.52601	7.49526	39.53472	7.51895	38.56547	4.88297	37.19364	1.15214	38.19671	3.88010	37.05896	0.78585	37.10298	0.90558	37.10993	0.92447	36.90653	0.37132
2018	36.91000	41.40229	12.17092	41.41118	12.19503	40.14842	8.77382	38.27999	3.71169	39.73235	7.64657	38.07588	3.15870	38.06567	3.13105	38.13348	3.31475	37.75671	2.29398
2019	37.25000	43.36763	16.42318	43.37671	16.44756	41.78659	12.17875	39.34982	5.63711	41.32284	10.93379	39.07286	4.89359	38.99424	4.68253	39.13784	5.06803	38.50500	3.36914
2020	36.26000	45.42627	25.27930	45.43554	25.30484	43.48249	19.91861	40.40340	11.42690	42.97108	18.50821	40.05109	10.45530	39.89046	10.01229	40.12412	10.65670	39.13309	7.92357
2021	37.52000	47.58264	26.81940	47.59208	26.84455	45.23867	20.57215	41.44095	10.45029	44.68000	19.08314	41.01164	9.30607	40.75607	8.62491	41.09330	9.52372	39.61944	5.59552
2022	39.13000	49.84136	27.37378	49.85097	27.39835	47.05774	20.26000	42.46273	8.51706	46.45257	18.71344	41.95548	7.22075	41.59280	6.29389	42.04630	7.45285	39.93878	2.06692
MAPE$_{pre}$			17.11450		17.13893		12.69909		5.88536		11.45465		5.18789		4.84487		5.33010		**3.17936**

4.2.3 Case III: Forecasting primary energy consumption in the Africa.

The energy consumption data in the Middle East from 2000 to 2022 were utilized. Among them, data from 2000 to 2015 were employed to construct the grey model and perform parameter estimation, while data from 2016 to 2022 were used to test its out-of-sample performance. All predicted values of the primary energy consumption in the Middle East are illustrated in Figure 6. Table 6 provides the evaluation metrics of the sample population. Table 7 lists the detailed results of the model predictions. The particle swarm optimization algorithm was employed to optimize the model parameters, and the optimization results are shown in Figure 5.

From Figure 5, it can be observed that after parameter optimization, the MAPE$_{fit}$ of the model reached optimal values, with the FAGM(1, 1, t^{α}) model having the lowest MAPE$_{fit}$, while the FTDGM(1, 1) model's MAPE$_{fit}$ was close to that of FDGM(1, 1), SFAGM(1, 1), and FGM(1, 1) models. As shown in Figure 6, the original data exhibited certain fluctuations. In out-of-sample predictions, all eight competing models gradually diverged from the original data, but the FTDGM(1, 1) model consistently maintained good performance, closely tracking the original data trend.

Table 6 shows that the evaluation metrics of the FTDGM(1, 1) model are significantly lower than those of other models. Specifically, the Pibas of the FTDGM(1, 1) model is 0.00054, which is the only value with an absolute magnitude less than 0.001, and other indicator values are also much lower than those of other competing models. From Table 7, it can be seen that the out-of-sample MAPE$_{pre}$ of the FTDGM model is the lowest at 1.77%, and it is the only model with an out-of-sample MAPE value less than 2%. Similarly, the FAGM(1, 1, t^{α}) model suffers from overfitting issues. Upon observing Table 7, it is apparent that at certain times, the point error of the FTDGM(1, 1) model is greater than that of other models, but its point error remains stable within a certain range, while the point errors of other models fluctuate greatly, leading to larger final out-of-sample MAPE$_{pre}$ values. Therefore, in this case, the FTDGM(1, 1) model demonstrates excellent out-of-sample predictive performance.

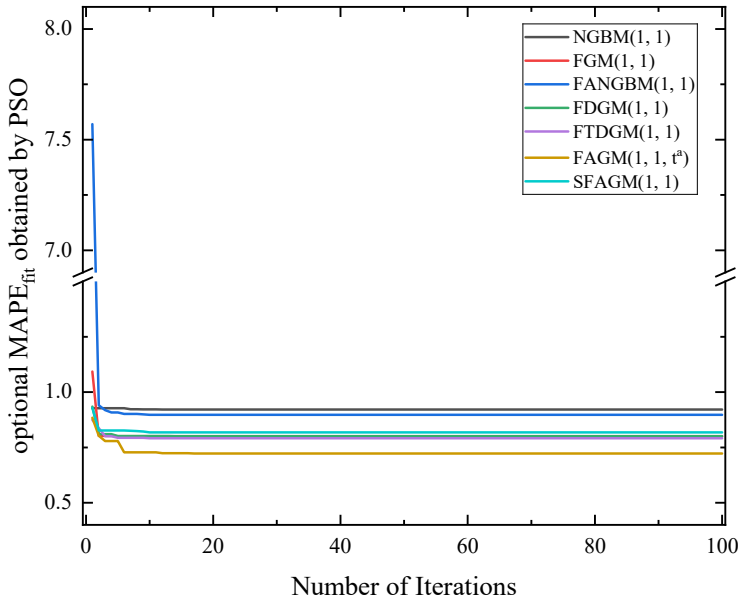

Figure 5. Optimal MAPE$_{fit}$ of model in Case III under PSO algorithm.

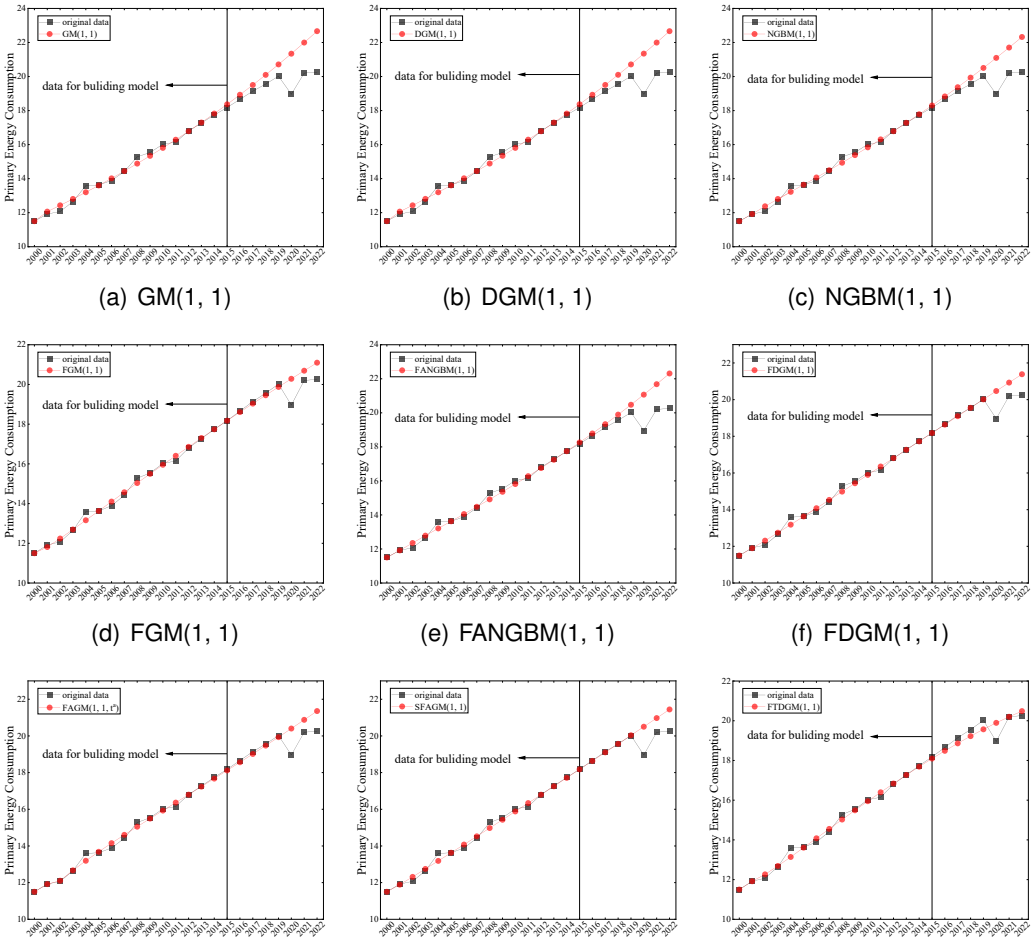

(a) GM(1, 1) (b) DGM(1, 1) (c) NGBM(1, 1)

(d) FGM(1, 1) (e) FANGBM(1, 1) (f) FDGM(1, 1)

(g) FAGM(1, 1, t^{α}) (h) SFAGM(1, 1) (i) FTDGM(1, 1)

Figure 6. Predicted values of all models in Case III.

Table 6. Overall-sample forecasting metrics for all models in Case III.

	ARE	MAE	MAPE	MPE	MAAPE	MSE	RMSE	RMSPE	SMAPE	U1	U2	AE	Pibas
GM(1, 1)	0.026219	0.475659	2.621928	-1.89501	0.026154	0.708965	0.842	0.043555	2.539706	0.025202	0.051097	-0.36782	-0.02215
DGM(1, 1)	0.026254	0.47626	2.625419	-1.90357	0.026189	0.709948	0.842584	0.043585	2.543001	0.025219	0.051132	-0.36918	-0.02223
NGBM(1, 1)	0.021788	0.39498	2.178826	-1.55648	0.021745	0.52372	0.723685	0.037522	2.117887	0.021713	0.043917	-0.30281	-0.01831
FGM(1, 1)	0.012369	0.212056	1.236891	-0.50396	0.012362	0.138126	0.371653	0.020309	1.223195	0.011235	0.022554	-0.09933	-0.00608
FANGBM(1, 1)	0.021133	0.383099	2.113254	-1.41045	0.021091	0.509964	0.714118	0.037023	2.05492	0.021443	0.043336	-0.27818	-0.01684
FDGM(1, 1)	0.013202	0.228679	1.320176	-0.70533	0.013191	0.196389	0.443158	0.023746	1.298794	0.013378	0.026893	-0.13737	-0.00839
FAGM(1, 1, t^{α})	0.013036	0.230944	1.303585	-0.58376	0.013026	0.180938	0.425368	0.022661	1.284073	0.012851	0.025814	-0.11558	-0.00707
SFAGM(1, 1)	0.013626	0.236582	1.362569	-0.72118	0.013613	0.209839	0.458082	0.024468	1.339685	0.013826	0.027799	-0.1414	-0.00863
FTDGM(1, 1)	**0.010894**	**0.183889**	**1.089439**	**0.038339**	**0.010892**	**0.077783**	**0.278896**	**0.015979**	**1.087835**	**0.008465**	**0.016925**	**0.00875**	**0.000539**

Table 7. Detailed results of sample predictions for all models in Case III.

	original data	GM(1, 1)		DGM(1, 1)		NGBM(1, 1)		FGM(1, 1)		FANGBM(1, 1)		FDGM(1, 1)		FAGM(1, 1, t^{α})		SFAGM(1, 1)		FTDGM(1, 1)	
		value	error(%)	value	error(%)	value	error(%)	value	error(%)	value	error(%)	value	error(%)	value	error(%)	value	error(%)	value	error(%)
2000	11.50000	11.50000	0.00000	11.50000	0.00000	11.50000	0.00000	11.50000	0.00000	11.50000	0.00000	11.50000	0.00000	11.50000	0.00000	11.50000	0.00000	11.50000	0.00000
2001	11.92000	12.06322	1.20148	12.06466	1.21356	11.92000	0.00000	11.81459	0.88434	11.91693	0.02573	11.89789	0.18550	11.92000	0.00000	11.89087	0.24439	11.92000	0.00000
2002	12.07000	12.43098	2.99071	12.43243	3.00270	12.37542	2.53042	12.23968	1.40579	12.35478	2.35940	12.31042	1.99187	12.10275	0.27134	12.31355	2.01783	12.26622	1.62571
2003	12.65000	12.80995	1.26444	12.81140	1.27593	12.80290	1.20872	12.69480	0.35414	12.78484	1.06596	12.74237	0.73016	12.67084	0.16476	12.74717	0.76815	12.68897	0.30808
2004	13.59000	13.20048	2.86624	13.20194	2.85550	13.22278	2.70211	13.16087	3.15767	13.20830	2.80871	13.18356	2.99073	13.19371	2.91606	13.18665	2.96801	13.14242	3.29345
2005	13.63000	13.60291	0.19875	13.60437	0.18801	13.64281	0.09395	13.63061	0.00449	13.63000	0.00000	13.63000	0.00000	13.68399	0.39613	13.63000	0.00000	13.60951	0.15032
2006	13.89000	14.01761	0.91873	14.01908	0.92929	14.06688	1.27341	14.10055	1.51582	14.05373	1.17875	14.07974	1.36603	14.15270	1.89126	14.07626	1.34098	14.08189	1.38148
2007	14.42000	14.44496	0.17306	14.44642	0.18324	14.49732	0.53618	14.56880	1.03187	14.48221	0.43141	14.53171	0.77466	14.60716	1.29792	14.52490	0.72744	14.55472	0.93426
2008	15.28000	14.88533	2.58293	14.88680	2.57332	14.93568	2.25339	15.03425	1.60832	14.91747	2.37260	14.98524	1.92908	15.05237	1.48976	14.97558	1.99230	15.02486	1.66975
2009	15.54000	15.33913	1.29263	15.34059	1.28319	15.38311	1.00960	15.49622	0.28173	15.36107	1.15142	15.43991	0.64409	15.49182	0.31006	15.42809	0.72015	15.49006	0.32138
2010	16.02000	15.80676	1.33111	15.80822	1.32196	15.84049	1.12053	15.95426	0.41033	15.81428	1.28412	15.89543	0.77759	15.92808	0.57377	15.88229	0.85960	15.94856	0.44597
2011	16.15000	16.28864	0.85848	16.29011	0.86754	16.30857	0.98189	16.40809	1.59810	16.27818	0.79370	16.35160	1.24829	16.36310	1.31952	16.33808	1.16461	16.39891	1.54122
2012	16.80000	16.78522	0.08795	16.78668	0.07928	16.78801	0.07138	16.85751	0.34234	16.75370	0.27561	16.80826	0.04919	16.79839	0.00957	16.79539	0.02743	16.83984	0.23716
2013	17.27000	17.29694	0.15600	17.29839	0.16440	17.27938	0.05429	17.30240	0.18758	17.24167	0.16402	17.26531	0.02714	17.23516	0.20173	17.25416	0.09171	17.27020	0.00114
2014	17.74000	17.82426	0.47497	17.82570	0.48310	17.78323	0.24367	17.74266	0.01500	17.74289	0.01628	17.72266	0.09772	17.67440	0.36976	17.71435	0.14457	17.68887	0.28823
2015	18.18000	18.36765	1.03220	18.36908	1.04007	18.30008	0.66049	18.17826	0.00957	18.25807	0.42944	18.18025	0.00137	18.11695	0.34680	18.17594	0.02235	18.09478	0.46873
MAPE$_{fit}$			1.08936		1.09132		0.92125		0.80044		0.89732		0.80084		**0.72240**		0.81809		0.79168
2016	18.66000	18.92761	1.43416	18.92903	1.44176	18.83043	0.91334	18.60917	0.27240	18.78793	0.68561	18.63802	0.11781	18.56351	0.51708	18.63889	0.11315	18.48688	0.92776
2017	19.14000	19.50465	1.90515	19.50605	1.91248	19.37478	1.22662	19.03538	0.54660	19.33316	1.00919	19.09592	0.23028	19.01470	0.65463	19.10319	0.19234	18.86408	1.44160
2018	19.56000	20.09927	2.75699	20.10066	2.76409	19.93360	1.91002	19.45690	0.52711	19.89442	1.70971	19.55394	0.03098	19.47107	0.45466	19.56882	0.04509	19.22528	1.71125
2029	20.02000	20.71202	3.45664	20.71339	3.46347	20.50739	2.43450	19.87374	0.73059	20.47239	2.25967	20.01204	0.03977	19.93309	0.43411	20.03578	0.07881	19.56935	2.25098
2020	18.96000	21.34345	12.57094	21.34480	12.57804	21.09662	11.26912	20.28592	6.99325	21.06773	11.11672	20.47019	7.96515	20.40122	7.60136	20.50405	8.14373	19.89513	4.93212
2021	20.20000	21.99413	8.88183	21.99545	8.88838	21.70180	7.43467	20.69348	2.44295	21.68112	7.33230	20.92839	3.60588	20.87585	3.34579	20.97363	3.82987	20.20138	0.00685
2022	20.26000	22.66465	11.86894	22.66594	11.87534	22.32342	10.18469	21.09644	4.12851	22.31325	10.13450	21.38661	5.56075	21.35737	5.41642	21.44452	5.84659	20.48684	1.11963
MAPE$_{pre}$			6.12495		6.13194		5.05328		2.23449		4.89253		2.50723		2.63201		2.60708		**1.77003**

4.3 Discussions

Through in-depth discussion of three cases, it is evident that the FTDGM(1, 1) model excels in maintaining close alignment with the original data. This implies its capability to effectively capture features and patterns within the data, thus enabling more accurate predictions. Compared to other models, FTDGM(1, 1) model consistently outperforms in out-of-sample predictions, showcasing its strong generalization ability to maintain robust predictive performance when faced with new data. Across the entire sample, FTDGM(1, 1) model exhibits superior evaluation metrics compared to other grey models. This underscores its prowess in predictive accuracy and overall performance. The following analysis will delve deeper into the predictive capacity and practical performance of this model.

4.3.1 Comparison between the FTDGM(1, 1) model and some linear models

In all three cases, the FTDGM(1, 1) model consistently demonstrates superior predictive performance compared to other linear grey system models, both in-sample and out-of-sample. Taking Case 4.2.1 as an example, the GM(1, 1) model exhibits fitting errors (MAPE$_{fit}$) and prediction errors (MAPE$_{pre}$) of 1.429% and 17.667% respectively, while the DGM(1, 1) model shows fitting errors (MAPE$_{fit}$) and prediction errors (MAPE$_{pre}$) of 1.431% and 17.667%. In contrast, the FTDGM(1, 1) model displays significantly lower fitting errors (MAPE$_{fit}$) and prediction errors (MAPE$_{pre}$) of 0.875% and 4.496% respectively. Similarly, in Case 4.2.2 and Case 4.2.3, the FTDGM(1, 1) model also demonstrates lower fitting errors (MAPE$_{fit}$) and prediction errors (MAPE$_{pre}$), ranging from 0.596% to 0.792% for fitting errors (MAPE$_{fit}$) and from 1.770% to 3.179% for prediction errors (MAPE$_{pre}$).

These results underscore the FTDGM(1, 1) model's advantage in maintaining robust predictive performance, particularly in out-of-sample predictions. It is noteworthy that the linear models exhibit

larger and less stable point errors in-sample, leading to relatively poorer out-of-sample predictive performance. Therefore, compared to linear grey system models, the FTDGM(1, 1) model showcases stronger generalization capabilities and more accurate predictive performance, providing reliable support for practical applications.

4.3.2 Comparison between the FTDGM(1, 1) model and some nonlinear models

In terms of out-of-sample predictive performance, the FTDGM(1, 1) model consistently demonstrates outstanding predictive capability across three different cases. Examining the convergence curves of MAPE$_{fit}$ in these cases, it is evident that the MAPE$_{fit}$ values of the FAGM(1, 1, t^{α}) model are consistently lower than those of the FTDGM(1,1) model. However, it is noteworthy that despite the lower fitting error exhibited by the FAGM(1, 1, t^{α}) model, the FTDGM(1, 1) model outperforms it in terms of out-of-sample MAPE$_{pre}$. This phenomenon strongly suggests the possibility of overfitting in the FAGM(1, 1, t^{α}) model.

In the three cases, the out-of-sample MAPE$_{pre}$ for the FTDGM(1, 1) model are 4.496%, 3.179%, and 1.770%, respectively. Compared to other nonlinear grey system models, the FTDGM(1, 1) model exhibits relatively stable errors at each point, avoiding sudden spikes in error, which is a significant advantage. Interestingly, for data with certain fluctuation characteristics, the FTDGM(1, 1) model consistently captures trends more accurately, resulting in predicted values that closely align with the original data, a feat that other competing models struggle to achieve. Therefore, the FTDGM(1, 1) model stands out in terms of out-of-sample predictive performance, particularly in stability and adaptability to data with fluctuating patterns.

5 Conclusions

This study employed the fractional time delayed grey model (FTDGM(1, 1)) to forecast the primary energy consumption in South and Central America, the Middle East, and the Africa. By utilizing thirteen comprehensive evaluation criteria, the performance of eight different grey system models was compared, and model parameters were optimized using the particle swarm optimization algorithm. The results clearly indicate that most linear grey system models perform poorly in these scenarios. While some nonlinear grey models outperform linear ones in terms of performance, their out-of-sample errors (MAPE$_{pre}$) are still significantly higher than those of the FTDGM(1, 1) model.

In comparison to the other eight grey models, the FTDGM(1, 1) model exhibited superior performance, further validating the feasibility of this modeling approach in constructing accurate grey system models. The findings suggest that the FTDGM(1, 1) model holds promise as a reliable decision support tool for future energy forecasting. The potential applications of this achievement are extensive, as it can contribute to advancing decision-making and management in the energy sector, providing robust support for the development of related industries.

References

[1] D Kamani and MM Ardehali. Long-term forecast of electrical energy consumption with considerations for solar and wind energy sources. *Energy*, 268:126617, 2023.

[2] Shahid Iqbal and Hafiza Iram Naseem. Energy consumption, carbon emissions, and economic growth in pakistan: A comprehensive analysis of long-term relations and short-term dynamics. *Qlantic Journal of Social Sciences and Humanities*, 4(3):215–221, 2023.

[3] OY Edelenbosch, K Kermeli, W Crijns-Graus, E Worrell, R Bibas, B Fais, S Fujimori, P Kyle, F Sano, and DP Van Vuuren. Comparing projections of industrial energy demand and greenhouse gas emissions in long-term energy models. *Energy*, 122:701–710, 2017.

[4] Azim Heydari, Farshid Keynia, Davide Astiaso Garcia, and Livio De Santoli. Mid-term load power forecasting considering environment emission using a hybrid intelligent approach. In *2018 5th International Symposium on Environment-Friendly Energies and Applications (EFEA)*, pages 1–5. IEEE, 2018.

[5] Jinhua Du, Qingyu Zheng, and Yuqing Wang. Mid-term and long-term prediction of carbon emissions in jiangsu province based on pca-stirpat improved ga-bp. In *2021 2nd International Conference on Intelligent Computing and Human-Computer Interaction (ICHCI)*, pages 1–7. IEEE, 2021.

[6] Ashoke Kumar Biswas, Sina Ibne Ahmed, Temitope Bankefa, Prakash Ranganathan, and Hossein Salehfar. Performance analysis of short and mid-term wind power prediction using arima and hybrid models. In *2021 IEEE Power and Energy Conference at Illinois (PECI)*, pages 1–7. IEEE, 2021.

[7] Guohui Li, Zelin Yang, and Hong Yang. A new hybrid short-term carbon emissions prediction model for aviation industry in china. *Alexandria Engineering Journal*, 68:93–110, 2023.

[8] Wei Sun and Chumeng Ren. Short-term prediction of carbon emissions based on the eemd-psobp model. *Environmental Science and Pollution Research*, 28(40):56580–56594, 2021.

[9] Hongyan Li, Bin Li, and Dongxiao Niu. Prediction on the energy consumption structure in liaoning province based on system dynamics. *POLISH JOURNAL OF ENVIRONMENTAL STUDIES*, 30(6):5593–5604, 2021.

[10] Steven P. Schnaars. How to develop and use scenarios. *Long Range Planning*, 20(1):105–114, 1987.

[11] Kathia Pinzón. Dynamics between energy consumption and economic growth in ecuador: A granger causality analysis. *Economic Analysis and Policy*, 57:88–101, 2018.

[12] Wei Cai, Kee hung Lai, Conghu Liu, Fangfang Wei, Minda Ma, Shun Jia, Zhigang Jiang, and Li Lv. Promoting sustainability of manufacturing industry through the lean energy-saving and emission-reduction strategy. *Science of The Total Environment*, 665:23–32, 2019.

[13] Deng Ju-Long. Control problems of grey systems. *Systems & Control Letters*, 1(5):288–294, 1982.

[14] Zheng-Xin Wang, Zhi-Wei Wang, and Qin Li. Forecasting the industrial solar energy consumption using a novel seasonal gm (1, 1) model with dynamic seasonal adjustment factors. *Energy*, 200:117460, 2020.

[15] Min Xia and Wai Keung Wong. A seasonal discrete grey forecasting model for fashion retailing. *Knowledge-Based Systems*, 57:119–126, 2014.

[16] Huiping Wang and Zhun Zhang. Forecasting per capita energy consumption in china using a spatial discrete grey prediction model. *Systems*, 11(6):285, 2023.

[17] Lifeng Wu, Sifeng Liu, Ligen Yao, Shuli Yan, and Dinglin Liu. Grey system model with the fractional order accumulation. *Communications in Nonlinear Science and Numerical Simulation*, 18(7):1775–1785, 2013.

[18] Wenqing Wu, Xin Ma, Bo Zeng, Yong Wang, and Wei Cai. Forecasting short-term renewable energy consumption of china using a novel fractional nonlinear grey bernoulli model. *Renewable Energy*, 140:70–87, 2019.

[19] Xin Ma, Xie Mei, Wenqing Wu, Xinxing Wu, and Bo Zeng. A novel fractional time delayed grey model with grey wolf optimizer and its applications in forecasting the natural gas and coal consumption in chongqing china. *Energy*, 178:487–507, 2019.

[20] Nai ming Xie and Si feng Liu. Discrete grey forecasting model and its optimization. *Applied Mathematical Modelling*, 33(2):1173–1186, 2009.

[21] Chun-I Chen, Hong Long Chen, and Shuo-Pei Chen. Forecasting of foreign exchange rates of taiwan's major trading partners by novel nonlinear grey bernoulli model ngbm(1,1). *Communications in Nonlinear Science and Numerical Simulation*, 13(6):1194–1204, 2008.

[22] Wei Meng, Daoli Yang, and Hui Huang. Prediction of china's sulfur dioxide emissions by discrete grey model with fractional order generation operators. *Complexity*, 2018:1–13, 2018.

[23] Wenqing Wu, Xin Ma, Yuanyuan Zhang, Yong Wang, and Xinxing Wu. Analysis of novel fagm (1, 1, tα) model to forecast health expenditure of china. *Grey Systems: Theory and Application*, 9(2):232–250, 2019.

[24] Jie Xia, Xin Ma, and Wenqing Wu. Fagm(1,1) model based on simpson formula and its application. *Chinese Management Science*, 29(05):240–248, 2021.